

# Journal of Biomedical Optics

BiomedicalOptics.SPIEDigitalLibrary.org

## Development of a reliable and reproducible phantom manufacturing method using silica microspheres in silicone

Charlotte J. Maughan Jones  
Peter R. T. Munro

**SPIE.**

Charlotte J. Maughan Jones, Peter R. T. Munro, "Development of a reliable and reproducible phantom manufacturing method using silica microspheres in silicone," *J. Biomed. Opt.* **22**(9), 095004 (2017), doi: 10.1117/1.JBO.22.9.095004.

# Development of a reliable and reproducible phantom manufacturing method using silica microspheres in silicone

Charlotte J. Maughan Jones<sup>a,\*</sup> and Peter R. T. Munro<sup>a,b</sup>

<sup>a</sup>University College London, Department of Medical Physics and Biomedical Engineering, London, United Kingdom

<sup>b</sup>The University of Western Australia, School of Electrical, Electronic and Computer Engineering, Crawley, Western Australia, Australia

**Abstract.** Optically scattering phantoms composed of silica microspheres embedded in an optically clear silicone matrix were manufactured using a previously developed method. Multiple problems, such as sphere aggregation, adsorption to the cast, and silicone shrinkage, were, however, frequently encountered. Solutions to these problems were developed and an improved method, incorporating these solutions, is presented. The improved method offers excellent reliability and reproducibility for creating phantoms with uniform scattering coefficient. We also present evidence of decreased sphere aggregation. © The Authors. Published by SPIE under a Creative Commons Attribution 3.0 Unported License. Distribution or reproduction of this work in whole or in part requires full attribution of the original publication, including its DOI. [DOI: [10.1117/1.JBO.22.9.095004](https://doi.org/10.1117/1.JBO.22.9.095004)]

Keywords: optical scattering; spectrophotometry; phantoms; Mie theory.

Paper 170365TNR received Jun. 7, 2017; accepted for publication Aug. 28, 2017; published online Sep. 18, 2017.

## 1 Introduction

Phantoms are integral in developing and refining biomedical imaging techniques as well as in system performance optimization. Phantoms for optical imaging often consist of a bulk material [e.g., silicone, epoxy resin, and poly(vinyl alcohol)], with or without embedded scatterers (e.g., Intralipid<sup>®</sup>, inorganic powders, and microspheres) and absorbers (e.g., India ink), allowing fine-tuning of the optical scattering and absorption properties of the sample as required for the intended application.<sup>1,2</sup> Silicone rubber is an inorganic, optically clear, and deformable bulk material and has had a variety of scattering and absorbing materials embedded within it, including absorbers, such as coffee, nigrosin, and India ink,<sup>3</sup> and scatterers, such as titanium dioxide,<sup>4</sup> barium sulfate powder,<sup>5</sup> polystyrene microspheres, and aluminum oxide<sup>6</sup> and, more recently, silica microspheres.<sup>5,7,8</sup> Despite their high cost, silica microspheres have become increasingly popular for use within phantoms<sup>5,7–10</sup> as the concentration required to achieve a designed scattering coefficient is easily calculated using Mie and continuum theory.<sup>11</sup> However, their use can be problematic due to the electrostatic forces that exist between them, causing significant sphere aggregation, which is more acute for smaller diameter spheres.<sup>12</sup> Methods have previously been presented that go some way to prevent this problem via stirring<sup>9</sup> or the use of hexane and an ultrasonic bath.<sup>7,8,10</sup> The procedure presented by Bisailon et al.<sup>7</sup> for incorporating silica microspheres into silicone rubber is considered a robust method for producing phantoms with homogeneously distributed microspheres, however alternative, often simpler methods for producing such phantoms have also been presented.<sup>5,6,8</sup> In this study, we present an existing method used by Curatolo et al.<sup>13</sup> and discuss the problems encountered during its implementation. We devised an

improved method to overcome the problems encountered during the implementation of the original method. All difficulties encountered during the development of the improved method and their solutions are discussed in detail.

Although a detailed discussion of the optical properties of tissue-mimicking phantoms is beyond the scope of this technical note, we briefly introduce the most significant properties and direct readers to a review paper for further details.<sup>11</sup> Neglecting absorption, the optical properties of such phantoms are usually described by the wavelength-dependent scattering coefficient  $\mu_s$  ( $\text{mm}^{-1}$ ) and anisotropy factor  $g$ . For phantoms composed of discrete scatterers,  $\mu_s$  is the product of scatterer concentration and scattering cross section, assuming a uniform scatterer distribution, and  $g$  is the average cosine of the angle by which particle ensembles scatter light. The reduced scattering coefficient is defined as  $\mu_s' = \mu_s(1 - g)$  and is applicable in the multiple scattering regime. The values of scattering cross section and  $g$  are easily calculated as a function of wavelength for spherical scatterers using Mie theory,<sup>14</sup> thus allowing  $\mu_s$  to be freely chosen for a single wavelength by varying the concentration.

## 2 Methods

### 2.1 Materials

The initial phantom manufacturing method used (from here on denoted the “original method”) was developed and successfully employed by Curatolo et al.<sup>13</sup> The improved method was subsequently established after problems were encountered during implementation of the original method. All phantoms made using the original and improved methods were constructed using silica microspheres of 1- $\mu\text{m}$  diameter, (Monospher<sup>®</sup> 1000, Merck, Darmstadt, Germany) embedded within a 2-part addition curing, room temperature vulcanizing silicone rubber Elastosil<sup>®</sup> RT 601 (Wacker Chemie AG, Munich, Germany). The silicone consists of a viscous, catalyst containing “silicone

\*Address all correspondence to: Charlotte J. Maughan Jones, E-mail: [rmapmau@ucl.ac.uk](mailto:rmapmau@ucl.ac.uk)

A" [platinum catalyst and polydimethylsiloxane (PDMS) polymer], which when mixed with "silicone B" (cross-linker and PDMS) forms an optically clear, deformable, and durable rubber through the cross-linking of PDMS. Silicone was chosen as the bulk material due to its optical clarity, durability, and long shelf life. Monodisperse spheres of a variety of diameters are commercially available. Spheres of 1- $\mu\text{m}$  diameter produce a tissue realistic  $g$  value when embedded in silicone<sup>11</sup> and were readily available in the laboratory, yet have a considerable tendency to aggregate, a problem that this report seeks to overcome. The manufacturer specified the refractive index of the cured silicone as 1.409 at a single wavelength of 589 nm.<sup>15</sup> The density of the cured silicone rubber was provided by the manufacturer as 1.02 g/ml.<sup>16</sup> The microsphere refractive index at a wavelength of 589 nm was not available from the manufacturer; therefore, the reference value for fused silica was assumed 1.4584.<sup>17</sup> From here on, without limiting the generality of the study, we consider the optical properties at a wavelength of 589 nm. This is sufficient to demonstrate the improvement (e.g., reducing sphere aggregation) offered by the presented phantom manufacturing method. The anisotropy factor ( $g$ ) for the silicone and 1- $\mu\text{m}$  sphere combination was calculated using the online Mie calculator, applicable to uniform scatterer distributions,<sup>14</sup> as 0.9533, which is independent of scatterer concentration.

## 2.2 Original Method

An overview of the original method is shown in Fig. 1. Stirring and sonication were used to create a homogenous sphere distribution, with the initial vacuum step used to remove air bubbles but also to aid the evaporation of hexane used to thin the silicone A. The ratio of 9:1 of silicone A:silicone B is recommended by the manufacturer. The casts were constructed using a soda lime glass slide and no. 2 cover slips as spacers, with a second slide being placed on top of the mixture to maintain a constant thickness and smooth surface. This phantom mixture can be cast into molds of any shape or size. The phantoms here were created with a thickness of  $\sim 200$  to  $400\ \mu\text{m}$ , specifically for analysis using a spectrophotometer with integrating sphere, where light loss from the sides of the phantoms should be minimized. Finally, it was assumed that all hexane had evaporated from the phantoms prior to curing and it had no effect on the curing process.

## 2.3 Improved Method

After the discovery of visible macroscopic sphere aggregates within the phantoms made using the original method, the following modifications were made to the manufacturing process to reduce aggregation:

- Increased time in ultrasound bath to 2 h in total.
- Ultrasound bath before vacuum so that silicone is at its lowest viscosity after hexane addition and again after vacuum to resuspend after period of static activity in the vacuum.
- Increased hexane (1:1 ratio silicone A:hexane) to reduce silicone viscosity and aid microsphere dispersion.

The increased proportion of hexane caused phantom swelling and subsequent shrinkage and adherence of the silicone to the slide. Hexane swells cured silicone;<sup>18</sup> however, once fully evaporated, the silicone shrinks and returns to its original size. Previous studies assumed that hexane had fully evaporated prior to curing.<sup>7,8,19</sup> This, however, appears to be untrue as swelling and subsequent shrinking are evident after curing, from visible marks on the phantom surface, formed by the uneven shrinking of the phantom leading to its pulling away from the cast in some areas. Although swelling cannot be entirely avoided, hexane can be encouraged to evaporate prior to curing. This can be done by increasing the time spent under vacuum to 2 h. Phantoms were also cured rapidly at  $70^\circ\text{C}$  for 10 min and immediately unmounted from their casts to avoid surface marks forming. While attempting to unmount the samples from their casts, it was noted that the increase in hexane also causes the sample to adhere to large areas of the slides on which they are cast, making them impossible to remove without damage.

Adherence of silicone to the glass slides was attributed to hydrogen bonding of silicone to the exposed silanol groups found on the surface of the soda lime glass,<sup>20,21</sup> previously discussed by Baxi et al.<sup>5</sup> who used trimethoxysilyloctane to reduce the hydrophilic nature of the glass surface. To overcome the problem of adherence, a simple glass passivation step was added: heating the slides to  $200^\circ\text{C}$  for 30 min prior to creating the casts. Heating catalyzes a dehydroxylation condensation reaction of the surface silanol groups, creating unreactive

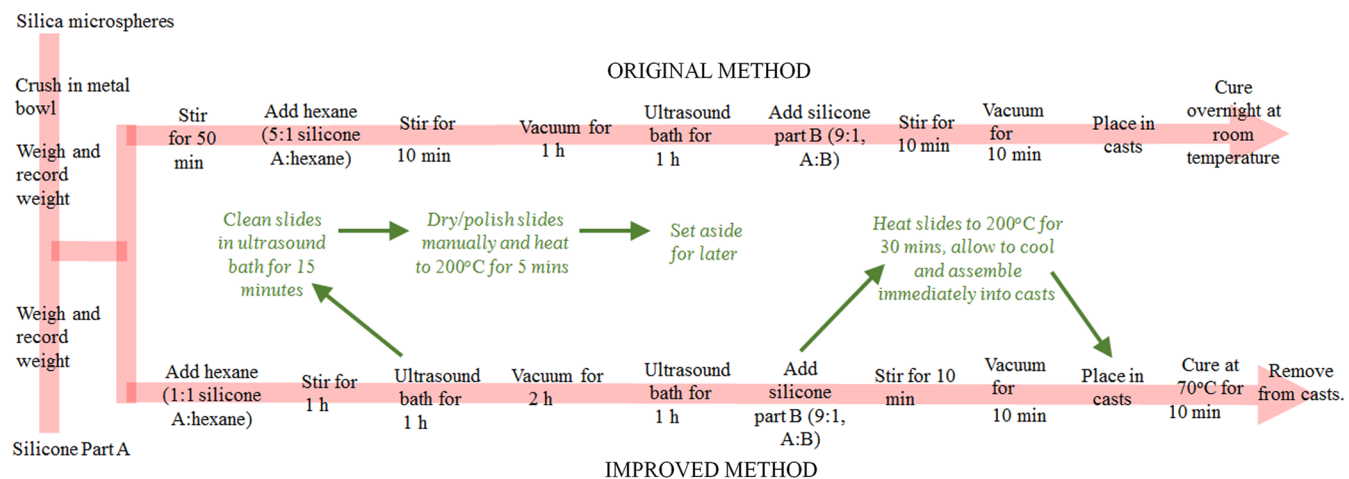


Fig. 1 Overview of original and improved methods.

siloxane bridges via the loss of a water molecule. Although heating to above 400°C, where stable siloxane bridges are formed would be optimal, equipment to reach this temperature was not available within the laboratory. Increasing the number of siloxane bridges found on the surface, even by a small amount, would disrupt the ideal one to one siloxane:silanol ratio required for effective adsorption. This surface modification can effectively be obtained at 200°C,<sup>22</sup> and this modification allowed the phantoms to be removed from their casts with ease and without damage to the phantom.

The above modifications were incorporated into the original method, yielding the improved method as shown in Fig. 1. These changes created a method with greater similarity to that presented by Bisaillon et al.<sup>7</sup> due to the greater volume of hexane and increased time under vacuum.

After removal from their casts, all phantoms made using the original and improved methods were mounted between two standard 1-mm-thick soda lime glass slides using small volumes of clear silicone. Mounting in this way creates a stable sample, with air free, refractive index matched contact between phantom and glass, ready for optical characterization via spectrophotometry.

A total of nine batches were made using the original method, of which five were immediately discarded due to visible macroscopic aggregation (see Fig. 2). In contrast, six batches were made using the improved method of which none contained macroscopic aggregation. Visual inspection thus provided the primary indication of the effectiveness of the improved method in comparison with the original method. Phantoms with visible air bubbles were also discarded. This initial quality control check for air bubbles and aggregates left batches containing either 1, 2, or 3 phantoms. Air bubbles were observed in phantoms created using both methods with equal frequency and were not considered a fault of the manufacturing method, but a randomly occurring problem during casting. Of the batches without macroscopic aggregation and air bubbles, only those with more than one phantom were considered (each batch represents a particular scattering concentration and multiple phantoms were made for each batch) and we denote these batches 1A, 1B, 1C, 2A, 2B, 2C, and 2D where prefixes 1 and 2 correspond to the original and improved methods, respectively.

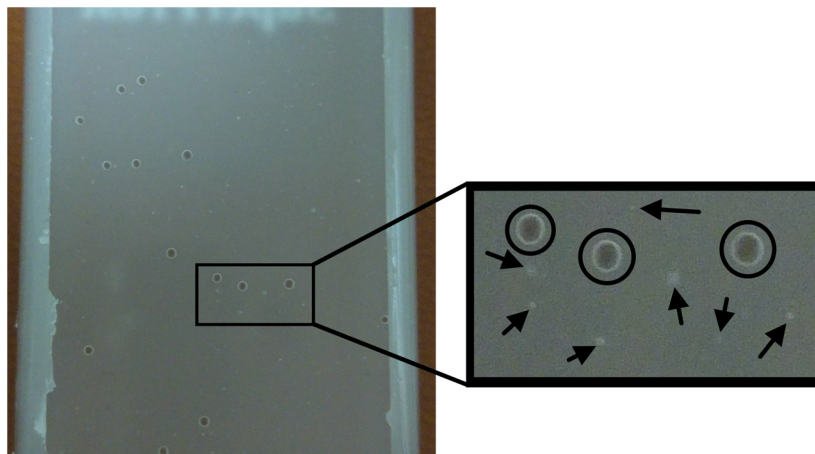


**Fig. 2** Example of discarded phantom made using method 1: arrows indicate macroscopic aggregates and circles highlight air bubbles.

### 3 Spectrophotometry

A PerkinElmer® Lambda 750 dual-beam spectrophotometer with 100-mm single integrating sphere detector accessory was used along with the inverse adding doubling (IAD) algorithm<sup>23</sup> to measure  $\mu'_s$  of each phantom at 589 nm thus allowing  $\mu_s$  to be calculated with knowledge of  $g$  (Sec. 1). “Dual-beam corrections” were applied, and an error tolerance of 0.1 (an IAD-specific parameter<sup>23</sup>) was specified, as IAD did not converge at the standard lower error. This value specifies the error tolerated by the IAD program before it terminates and, therefore, determines the error in the calculated value of  $\mu'_s$ , with lower error values producing more accurate optical properties. The thickness of each sample was determined using digital calipers.

The percentage scatterer by weight represents the ratio of the mass of silica spheres compared to that of the silicone part A—both measured on a high precision balance (to 4 decimal places) during the manufacturing process. It was assumed that this ratio remained constant throughout the manufacturing process and, therefore, is representative of the scatterer density in the final cured phantom, however, due to the irreversible curing process, this assumption cannot be verified.

If the microspheres are uniformly dispersed within the silicone matrix, phantoms from the same batch should have nearly identical values of  $\mu_s$ . Variation in  $\mu_s$  among phantoms of the same batch, therefore, indicates aggregation has occurred within that batch.

Figure 3 shows that batches made using the original method exhibit greater variation in  $\mu_s$  than those made using the improved method, which all vary by  $<1 \text{ mm}^{-1}$  except batch 2C which has an intrabatch variation of  $2.2 \text{ mm}^{-1}$ . The variation demonstrated by batches made using the original method, 1B and 1C ( $4.80$  and  $5.83 \text{ mm}^{-1}$ , respectively), are over double that of the largest variation shown by the improved method.

As expected, phantoms from both methods demonstrate an approximately linear relationship between the scatterer concentration and  $\mu_s$ . This linear relationship appears stronger for the original method; however, intrabatch variation makes this difficult to judge. This linear relationship is expected to break down for high scatterer concentrations;<sup>24</sup> however, analysis of this is beyond the scope of this study since we are principally concerned with the reduction of sphere aggregation.

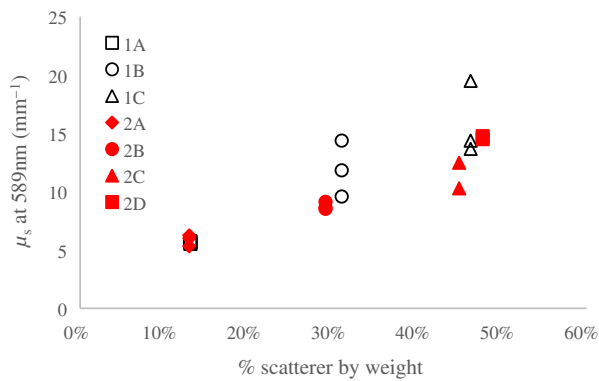


Fig. 3  $\mu_s$  values for all phantoms.

Three plain silicone phantoms made using method 2 were also measured; the value of  $\mu_s$  was  $0.004 \pm 0.006 \text{ mm}^{-1}$ , thus confirming that the manufacturing process has a negligible effect on the intrinsic scattering of silicone.

#### 4 Discussion

We believe that the elevated intrabatch variability in IAD calculated  $\mu_s$  values of the original method over the improved method is due to sphere aggregation. The number, size, and morphology of aggregates appear random, creating areas of higher and lower sphere density within the same phantom, yielding a nonuniform scattering coefficient throughout. This variation in sphere density within and among phantoms of the same batch causes large intrabatch variability. The decrease in  $\mu_s$  variation offered by the improved method, in addition to the visual improvement and significant reduction in the number of phantoms discarded, provides evidence that the improved method indeed results in a reduction in sphere aggregation. Quantification of this improvement would require a high-resolution imaging technique and a greater number of phantoms, which was beyond the scope of this study.

The swelling and subsequent shrinkage of the silicone observed during the development of the improved method suggest that the commonly stated assumption that hexane is evaporated before curing is incorrect. Further work is needed to determine whether a different solvent that does not cause swelling may be more appropriate, for example, tert-butyl alcohol,<sup>18</sup> however, steps discussed here go some way to reduce the effect of swelling and subsequent shrinkage on the physical properties of the phantom.

Although not explicitly considered here, the absorption coefficient ( $\mu_a$ ) was negligible for all phantoms. The highest calculated value of  $\mu_a$  (from IAD) was  $1.45 \times 10^{-3} \text{ mm}^{-1}$ —if considering the Beer–Lambert law, this equates to a 0.0289% reduction in beam intensity over a 0.2-mm distance, and therefore, the phantoms can be considered “scattering only.”

#### 5 Conclusion

The production of phantoms consisting of silicone rubber and 1- $\mu\text{m}$  diameter silica microspheres poses significant difficulty due to the predisposition of spheres to aggregate; however, steps can be taken to successfully reduce aggregation—predominantly due to the addition of a larger volume of hexane. Finally, a reproducible and highly reliable method of phantom manufacture has been presented in detail, which overcomes all

the problems encountered while using previously presented methods, as well as problems encountered during the development of the final improved method.

#### Disclosures

The authors have no relevant financial interests in this article and no potential conflicts of interest to disclose.

#### Acknowledgments

We acknowledge fruitful discussions with Dr. A. Curatolo. We are grateful to Miss L. An for her help with the spectrophotometer and IAD program. C.J.M.J. is supported by an Engineering and Physical Sciences Research Council (EPSRC) studentship (No. EP/M507970/1). P.R.T.M. is supported by a Royal Society University Research Fellowship (No. UF130304). This work was partially supported by EPSRC Grant No. EP/P005209/1.

#### References

- G. Lamouche et al., “Review of tissue simulating phantoms with controllable optical, mechanical and structural properties for use in optical coherence tomography,” *Biomed. Opt. Express* **3**(6), 1381–1398 (2012).
- B. W. Pogue and M. S. Patterson, “Review of tissue simulating phantoms for optical spectroscopy, imaging and dosimetry,” *J. Biomed. Opt.* **11**(4), 041102 (2006).
- R. B. Saager et al., “Multilayer silicone phantoms for the evaluation of quantitative optical techniques in skin imaging,” *Proc. SPIE* **7567**, 756706 (2010).
- C. Böcklin et al., “Mixing formula for tissue-mimicking silicone phantoms in the near infrared,” *J. Phys. D Appl. Phys.* **48**(10), 105402 (2015).
- J. Baxi et al., “Retina-simulating phantom for optical coherence tomography,” *J. Biomed. Opt.* **19**(2), 021106 (2014).
- R. Bays et al., “Three-dimensional optical phantom and its application in PDT,” *Lasers Surg. Med.* **21**(3), 227–234 (1997).
- C.-E. Bisailon et al., “Deformable and durable phantoms with controlled density of scatterers,” *Phys. Med. Biol.* **53**(13), N237–N247 (2008).
- D. Y. Diao et al., “Durable rough skin phantoms for optical modeling,” *Phys. Med. Biol.* **59**(2), 485–492 (2014).
- M. Firbank, M. Oda, and D. T. Delpy, “An improved design for a stable and reproducible phantom material for use in near-infrared spectroscopy and imaging,” *Phys. Med. Biol.* **40**, 955–961 (1995).
- M. R. N. Avnani et al., “Two applications of solid phantoms in performance assessment of optical coherence tomography systems,” *Appl. Opt.* **52**(29), 7054–7061 (2013).
- S. L. Jacques, “Optical properties of biological tissues: a review,” *Phys. Med. Biol.* **58**(11), R37–R61 (2013).
- Bangs Laboratories Inc., “TechNote 202—microsphere aggregation,” <http://www.bangslabs.com/support/technical-support/technotes> (2003).
- A. Curatolo et al., “Quantifying the influence of Bessel beams on image quality in optical coherence tomography,” *Sci. Rep.* **6**, 23483 (2016).
- S. A. Prahl, “Mie scattering calculator,” 2007, [http://omlc.ogi.edu/calc/mie\\_calc.html](http://omlc.ogi.edu/calc/mie_calc.html).
- Wacker Chemie AG, “Overview of Elastosil grades silicone rubber for the appliance industry,” [https://www.wacker.com/cms/media/publications/downloads/6009\\_EN.pdf](https://www.wacker.com/cms/media/publications/downloads/6009_EN.pdf).
- Wacker Chemie AG, “Technical data sheet for Elastosil® RT 601 A/B,” 2014, <https://www.wacker.com/cms/en/products/product/product.jsp?product=10461>.
- I. H. Malitson, “Interspecimen comparison of the refractive index of fused silica,” *J. Opt. Soc. Am.* **55**(10), 1205 (1965).
- J. H. Koschwaner, R. H. Carlson, and D. R. Meldrum, “Thin PDMS films using long spin times or tert-butyl alcohol as a solvent,” *PLoS One* **4**(2), e4572 (2009).
- A. Grimwood et al., “Elastographic contrast generation in optical coherence tomography from a localized shear stress,” *Phys. Med. Biol.* **55**(18), 5515–5528 (2010).

20. L. T. Zhuravlev, "The surface chemistry of amorphous silica. Zhuravlev model," *Colloids Surf. A* **173**(1–3), 1–38 (2000).
21. A. Rimola et al., "Silica surface features and their role in the adsorption of biomolecules: computational modeling and experiments," *Chem. Rev.* **113**(16), 4216–4313 (2013).
22. A. A. Christy, "Effect of heat on the adsorption properties of silica gel," *Int. J. Eng. Technol.* **4**(4), 484–488 (2012).
23. S. A. Prah, "Everything I think you should know about inverse adding doubling," <http://omlc.ogi.edu/software/iad> (2011).
24. C. F. Bohren and D. M. Huffman, *Absorption and Scattering of Light by Small Particles*, Wiley Interscience, New York (1983).

Biographies for the authors are not available.